PATENT CAUTION

ORNL--96020587

C/ORNL95-0330

ornl

OAK RIDGE NATIONAL LABORATORY

LOCKHEED MARTIN

Final Report for
Cooperative Research and Development
Agreement (CRADA) Number ORNL95-0330

Heat Transfer Surface Augmentation for Zeotropic Mixture Alternatives to HCFC Refrigerants

James C. Conklin
Oak Ridge National Laboratory

J. E. Bogart
Wolverine Tube, Inc.

MANAGED AND OPERATED BY
LOCKHEED MARTIN ENERGY RESEARCH CORPORATION
FOR THE UNITED STATES
DEPARTMENT OF ENERGY

ORNL-27 (3-96)

C/ORNL95-0330

Final Report for
Cooperative Research and Development
Agreement (CRADA) Number ORNL95-0330

HEAT TRANSFER SURFACE AUGMENTATION FOR ZEOTROPIC MIXTURE ALTERNATIVES TO HCFC REFRIGERANTS

James C. Conklin
Oak Ridge National Laboratory

J. E. Bogart
Wolverine Tube, Inc.

Prepared by the
Oak Ridge National Laboratory
Oak Ridge, Tennessee 37831
managed by
Lockheed Martin Energy Research Corporation
for the
U.S. Department of Energy
under contract DE-AC05-96OR22462

ABSTRACT

This paper reports an investigation of the phase-change heat transfer from three different enhanced surfaces on the inside of 5/16 inch diameter copper tubes manufactured by Wolverine Tube, Inc., of Decatur, Alabama. These enhanced surfaces are commonly called microfins, and the three tubes investigated had 40, 50, and 52 fins in cross-section. The evaporating and condensing heat transfer performance was measured for two refrigerants: pure R-410A and a zeotropic mixture called Q8 that has a high glide. The experiment was conducted in an apparatus consisting of a variable-speed compressor having a range of 500-3000 rpm and counterflow concentric tube heat exchangers. The refrigerant circulates inside the central tube and water circulates in the annulus.

For the tests in R-410A, the 40 and 52 fin surfaces had comparable condensing and evaporating heat transfer performance and both had higher heat transfer than the 50 fin surface. For the condensation tests in Q8, all three tube surfaces had approximately equal heat transfer performance. For the evaporation tests in Q8, the 50 and 40 fin tubes performed equally well in evaporation but the 52 fin tube showed slightly lower evaporating heat transfer performance. Although the amount of data scatter is substantial, the fin height appears to have had the most influential effect on the augmentation of heat transfer for both evaporation and condensation.

STATEMENT OF THE OBJECTIVES

The refrigeration industry has employed internally enhanced tubes to improve the performance of refrigeration machinery over the past few years. A popular internal tube enhancement, called "microfins," consist of extruding many small fins on the order of 0.010 inch in height during tube manufacture. Microfin enhanced tubes show significantly improved heat transfer with only a slight increase in pressure drop, hence the overall refrigeration system performance is improved. Many tube manufacturers sell different microfin designs, with such geometric differences as fin counts, fin heights and helix angles. Manufacturers are continually improving their products to meet new market requirements. One such new application of enhanced tubes may be zeotropic refrigerant mixtures (ZRM).

Oak Ridge National Laboratory (ORNL) has been investigating ZRMs as replacements for the refrigerants presently used in air conditioners and heat pumps. For ZRMs in the wet (two-phase) region, the saturation temperature at constant pressure varies with respect to quality, and thus the evaporation process is not isothermal. This nonisothermal phase-change behavior can improve the heat exchanger effectiveness of evaporators and condensers (Granryd and Conklin 1990) as well as the thermodynamic cycle efficiencies (McLinden and Radermacher 1987). However, other investigators (Jung et al. 1989; Ross et al. 1987) have measured heat transfer coefficients for binary ZRMs undergoing evaporation in smooth tubes that were less than the heat transfer coefficients for either of the pure constituent refrigerants. Kaul et al. (1996) also show degraded heat transfer coefficients for ZRMs in microfin tube geometries. Additional heat transfer area for ZRM evaporators and condensers would thus be required. Hence, the effect of different microfin enhanced surfaces on evaporating and condensing heat transfer was investigated here for two fluids: R-410A—a refrigerant believed to become the most likely replacement for R-22 in residential heat pumps and air conditioners, and Q8—an ORNL proprietary mixture of refrigerants having an approximately 20°F change in temperature from liquid to vapor.

All Wolverine copper tubes for this particular series of tests were 5/16 inch in outside diameter with a 0.012 inch wall thickness. The only differences were the fin height, the cross-section fin count, and the helix angle with respect to the tube centerline as described on the following table.

Protected CRADA Information		
Fin count	Fin height (inch)	Helix angle (°)
40	0.010	18
50	0.008	18
52	0.008	8

The 50 fin tube is presently sold by Wolverine, and other manufacturers sell tubes with essentially the same geometry for R-22 service. The 40 fin tube is a new proprietary product from Wolverine designed and tested for R-410A service. The 52 fin design has the same internal heat transfer area as the 50 fin, and was intended to show the effect of helix angle on phase-change heat transfer.

BENEFITS TO THE FUNDING DOE OFFICE'S MISSION

The information developed by this CRADA will directly benefit the DOE Office of Building Technologies mission for efficiency improvement of building heating and cooling equipment. The enhanced heat transfer surfaces researched here will result in more efficient heat exchangers for residential air conditioning and heat pump refrigeration machinery.

EXPERIMENTAL APPARATUS

The heat transfer from enhanced surfaces during tube-side refrigerant phase-change was investigated using a highly instrumented apparatus, shown in Figure 1, that consists of the following components: a variable-speed compressor having a range of 500-3000 rpm, which allows for variable heat exchanger loads; a variable-orifice refrigerant metering device (needle valve); and two sets of counterflow concentric-tube heat exchangers having two different enhanced tube-side surfaces. The refrigerant was circulated inside the central tube and water was circulated in the annulus. A variable-speed compressor was chosen to provide for different heat loads of the heat exchangers. A needle valve was chosen for flexibility in controlling refrigerant conditions: this flexibility is lacking in capillary tubes and thermal expansion valves. Since water-to-refrigerant heat exchangers were used in the experimental apparatus, the inlet water temperatures were selected to yield refrigerant saturation pressures equivalent to those determined for air-to-refrigerant heat exchangers in the U.S. Department of Energy standard rating conditions for heat pumps (Miller 1989).

The heat exchangers, with instrumentation as shown in Figure 2, consist of a central tube and an outer tube forming an annulus. There are eight horizontal passes where the outer surfaces of the water annulus and the refrigerant bends are insulated. The inner tube is copper and has an outer diameter of 0.3125 in. with a wall thickness of 0.012 in. The outer copper tube has an inner diameter of 0.524 in. Each horizontal heat transfer section is 82 inches in length.

TESTING PROCEDURE

The output of instrumentation such as mass flow meters, pressure transducers, and the thermocouples and resistance temperature devices (RTDs) shown in Figures 1 and 2 was recorded on a personal computer. Data were taken every 10 seconds and averaged over a 15-minute period during steady-state operation. All pressure transducers, flowmeters, thermocouples, and RTDs were calibrated prior to testing.

Water flow rates to the heat exchangers are pneumatically controlled to allow for rapid changes in test conditions. Inlet temperatures to the condenser are maintained with a mixing valve that introduces cool process water while bleeding off warmer water that has passed through the condenser. Inlet water temperatures to the evaporator are controlled by a bank of resistance heaters in the closed-loop system.

Test conditions were based on the U. S. Department of Energy standard rating conditions for an air-source heat pump. Inlet water temperatures were adjusted to yield refrigerant saturation pressures equivalent to those determined from previous testing with an air-source system (Miller 1989). The heat rates for the refrigerant side and the water side were determined from measured inlet and outlet temperatures and measured flow rates and then checked for a steady-state heat balance. The electrical power measurements for the closed-loop system were also used to check for a heat balance in steady-state operation. During the testing, minimal subcooling at the condenser exit and minimal superheating at the evaporator exit were maintained to ensure two-phase conditions in the heat exchangers. Only the heat transfer in the two-phase region of the heat exchangers is reported here.

The tests were performed with R-410A and Q8 at different compressor speeds with subsequent heat exchanger loads as a basis for comparison of the performance of the three tubes. Both R-410A and the Q8 mixture had an alkylbenzene oil present for lubrication of the compressor. The concentration of oil, which was not monitored during the tests, was on the order of 1%. The effect of oil on the heat transfer coefficient or pressure drop was not investigated.

For the capabilities of the experimental apparatus, the observed refrigerant mass flux in the condenser was typical of that seen in existing refrigeration devices. For simplicity, both the condenser and the evaporator were identical. As a result, the observed mass flux in the evaporator was more than twice that typically found in existing refrigeration devices. Consequently, the pressure drop in evaporation was substantially more than that tolerable in existing refrigeration machinery. The intent of this experimental investigation was to measure differences, if any, in heat transfer performance—any differences at high mass fluxes would be even greater at lower mass fluxes since all tubes appear to tend to the same heat transfer performance as the flow is increased to very high amounts.

The pressure drop of the overall heat exchanger was recorded during the tests, but is not reported here. There were many portions of the tube circuit that showed no heat transfer, thus the measured pressure drop would not be representative of the pressure drop in the active heat transfer region.

HEAT TRANSFER ANALYSIS

The condensing or evaporating heat transfer coefficient is computed from the measured temperatures and flows. First, a "standard" log mean temperature difference is computed from the measured evaporator inlet and outlet temperatures with the following equation:

$$T_{lmtd} = \frac{(T_{w,i} - T_{r,o}) - (T_{w,o} - T_{r,i})}{\ln\left(\frac{T_{w,i} - T_{r,o}}{T_{w,o} - T_{r,i}}\right)} , \qquad (1)$$

where T represents a temperature. Subscript r represents the refrigerant, w represents the water, i represents the corresponding flow inlet, and o represents the corresponding flow outlet.

The total heat flux to the refrigerant during the evaporation process is then determined from the measured water temperatures and flow rate with the following equation:

$$q'' = \frac{\dot{m}_w c_w (T_{w,i} - T_{w,o})}{A_w} , \qquad (2)$$

where A_w represents the heat transfer area of the outer surface of the refrigerant tube to the water. Heat gains from the environment were neglected because the outer annulus was insulated and the total heat rate transferred from the water was within 5% of the total heat rate transferred to the refrigerants for an acceptable test.

Axial heat losses along the copper tube were neglected in Equation (2). To justify this assumption, the ratio of the convection conductance ($U \times A_w$) and the axial thermal conductance ($k_{cu} \times A_{cu}/l$) was computed. This ratio was on the order of 3×10^4, indicating a much greater resistance to the flow of heat along the tube wall compared to the flow of heat convected to the fluids through the tube wall. Thus, axial heat transfer was neglected for computing the overall heat transfer coefficient.

An overall heat transfer coefficient is then determined as follows:

$$U = \frac{q''}{T_{lmtd}} . \qquad (3)$$

The heat transfer coefficient to the water was obtained from the following relationship:

$$h_w = \frac{k_w}{d_{hyd}} Nu_{pet} \frac{od_{ann}}{id_{ann}} , \qquad (4)$$

where Nu_{pet} represents the Nusselt number of the water annulus predicted by the Petukhov relation (Petukhov 1970). Viscosity variations were neglected because the difference in temperature between the tube wall and the water was less than 10 C° (18 F°). Use of this modified Petukhov relationship gave the best agreement with Wolverine's data for the 40 and 50 fin designs for the R-410A series of condensing tests.

The heat transfer coefficient of the refrigerant is then computed by the following equation:

$$h_r = \frac{1}{\frac{A_r}{A_w}\left(\frac{1}{U} - \frac{1}{h_w}\right)} , \tag{5}$$

where A_r represents the heat transfer area of the inner tube surface to the refrigerant. This area A_r is the inner tube area at the root of the fins. Thus, no surface area of the fins only is used in either the heat transfer measurements or the reported mass flux. Also, because the tubes were new, no fouling factor was assigned.

HEAT TRANSFER RESULTS

The condensing test results are presented in Figure 3 for R-410A. The measured condensing heat transfer coefficient for the 40 fin tube is in substantial agreement with test data from Wolverine Tube. The 50 fin data shown in Figure 3 are slightly lower than that measured by Wolverine. The 52 fin condensing data shown in Figure 3 appear to lie along the same line as the 40 fin.

The condensing test results are presented in Figure 4 for Q8. All three tubes appear to have essentially the same performance with respect to mass flux. All condensing heat transfer coefficients are approximately 20% lower than those for R-410A.

The evaporating test results are presented in Figure 5 for R-410A. As for the condensing tests in R-410A, the 40 fin tube and the 52 fin tube appear to have the same performance, although experimental data scatter is apparent. The 50 fin tube has an approximately 10% less heat transfer coefficient than the 40 fin or 52 fin. This decreased heat transfer coefficient of the 50 fin tube is consistent with data measured by Wolverine, although the Wolverine data for the 50 fin tube was 20% lower than that for the 40 fin. That Wolverine data, however, is at half of the observed mass fluxes shown here. In general, as the mass flux increases, the enhancement effects of any finned geometry tend to decrease.

The evaporating test results are presented in Figure 6 for Q8. The measured 40 fin heat transfer coefficients appear to lie along the same line as the 50 fin. The 52 fin data lie approximately 10% below that of the 40 and 50 fin data, although experimental data scatter is also apparent. The measured performance of Q8 in evaporation heat transfer is approximately 20-25% lower than that of R-410A.

INVENTIONS

There were no inventions developed during this CRADA.

COMMERCIALIZATION POSSIBILITIES

The enhanced heat transfer surfaces developed in this CRADA may be commercially developed as desired by Wolverine Tube, Inc., at their option.

PLANS FOR FUTURE COLLABORATION

Wolverine Tube, Inc., and Oak Ridge National Laboratory will continue their mutually beneficial collaboration for enhanced heat transfer surfaces for advanced refrigeration machinery.

CONCLUSIONS

For condensation heat transfer, the 52 fin tube had better performance than the 50 fin tube for R-410A, but no difference was measured in Q8. Because the 52 fin tube had the same surface area and fin height as the 50 fin tube but had a lower tube helix angle, a lower helix angle may be desirable for condensing R-410A . The higher fin height of the 40 fin tube may also favorably improve R-410A condensing heat transfer.

For evaporation heat transfer, the 52 fin tube had better performance than the 50 fin tube for R-410A, but 50 fin tube had better performance than the 52 fin tube for Q8. The reason for this contrary behavior is unknown. The 40 fin tube had the best evaporating heat transfer performance for both refrigerants.

Although the amount of data scatter is substantial, the fin height appears to have had the most influential effect of the augmentation of heat transfer in both evaporation and condensation.

REFERENCES

Granryd, E., and J. C. Conklin. 1990. Thermal performance analysis for heat exchangers using nonazeotropic refrigerant mixtures. *Heat transfer in advanced energy systems*. R. F. Boehm and G. Vliet, eds., HTD 151, AES 18. New York: The American Society of Mechanical Engineers.

Jung, D. S., M. O. McLinden, R. Radermacher, and D. A. Didion. 1989. Horizontal flow boiling heat transfer experiments with a mixture of R-22/R-114. *Int. J. Heat Mass Trans.*, 32: 131-145.

Kaul, M. P., M. A. Kedzierski, and D. A. Didion. 1996. Horizontal Flow Boiling of Alternative Refrigerants Within a Fluid Heated Micro-Fin Tube. *Process, Enhanced, and Multiphase Heat Transfer, A Festschrift for A. E.. Bergles*, R. M. Manglik and A. D. Krauss, eds., Begell House, New York, pp. 167–173.

McLinden, M. O., and R. Radermacher. 1987. Methods for comparing the performance of pure and mixed refrigerants in the vapour compression cycle. *Int. J. Refrigeration*, 10: 318-325.

Miller, W. A. 1989. Laboratory study of the dynamic losses of a single speed, split system air-to-air heat pump having tube and plate fin heat exchangers. ORNL/CON-253, Oak Ridge National Laboratory, Oak Ridge, Tennessee.

Petukhov, B. S. 1970. Heat Transfer and Friction in Turbulent Pipe flow with Variable Physical Properties. *Advances in Heat Transfer*, Vol. 6, J. P. Hartnett and T. F. Irvine, eds., Academic Press, New York, pp. 503–565.

Ross, H., R. Radermacher, M. DiMarzo, and D. A. Didion. 1987. Horizontal flow boiling of pure and mixed refrigerants. *Int. J. Heat Mass Trans.*, 30: 979-992.

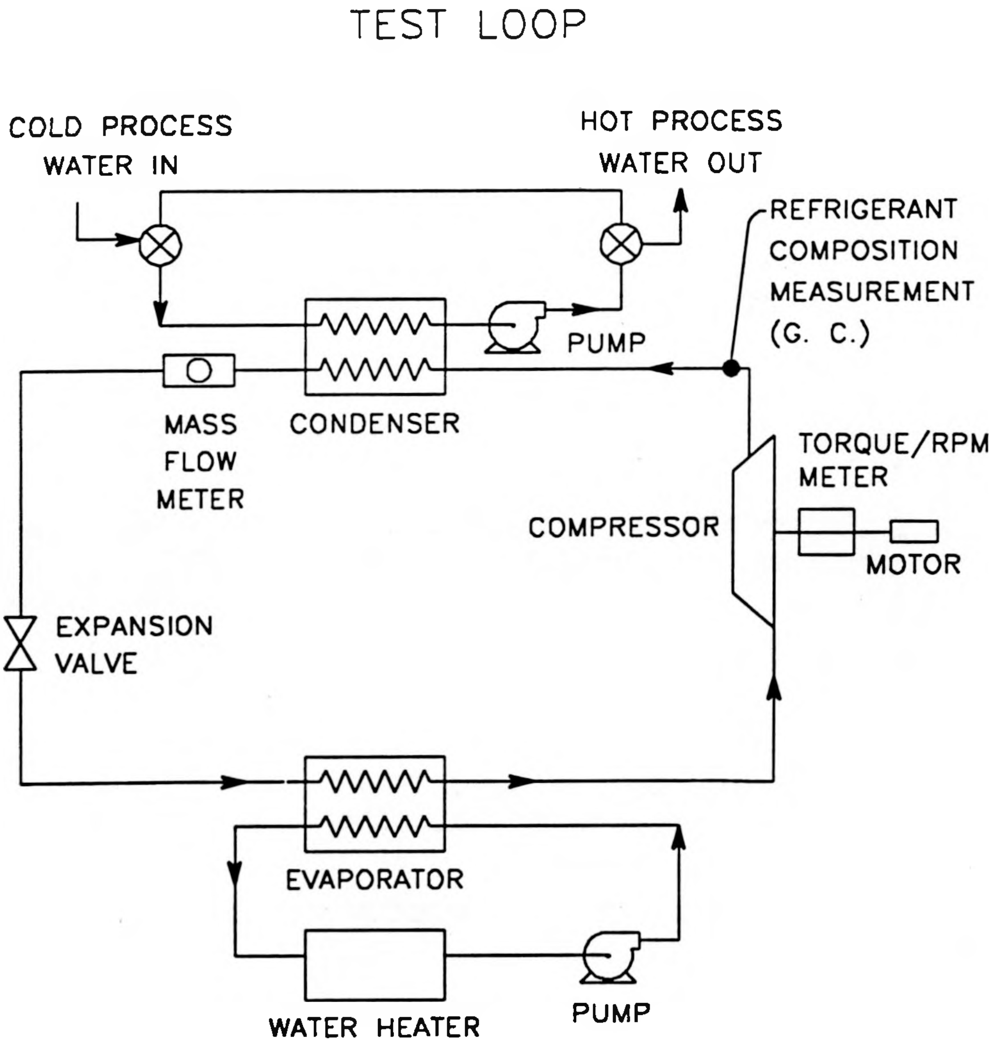

Figure 1. Test apparatus.

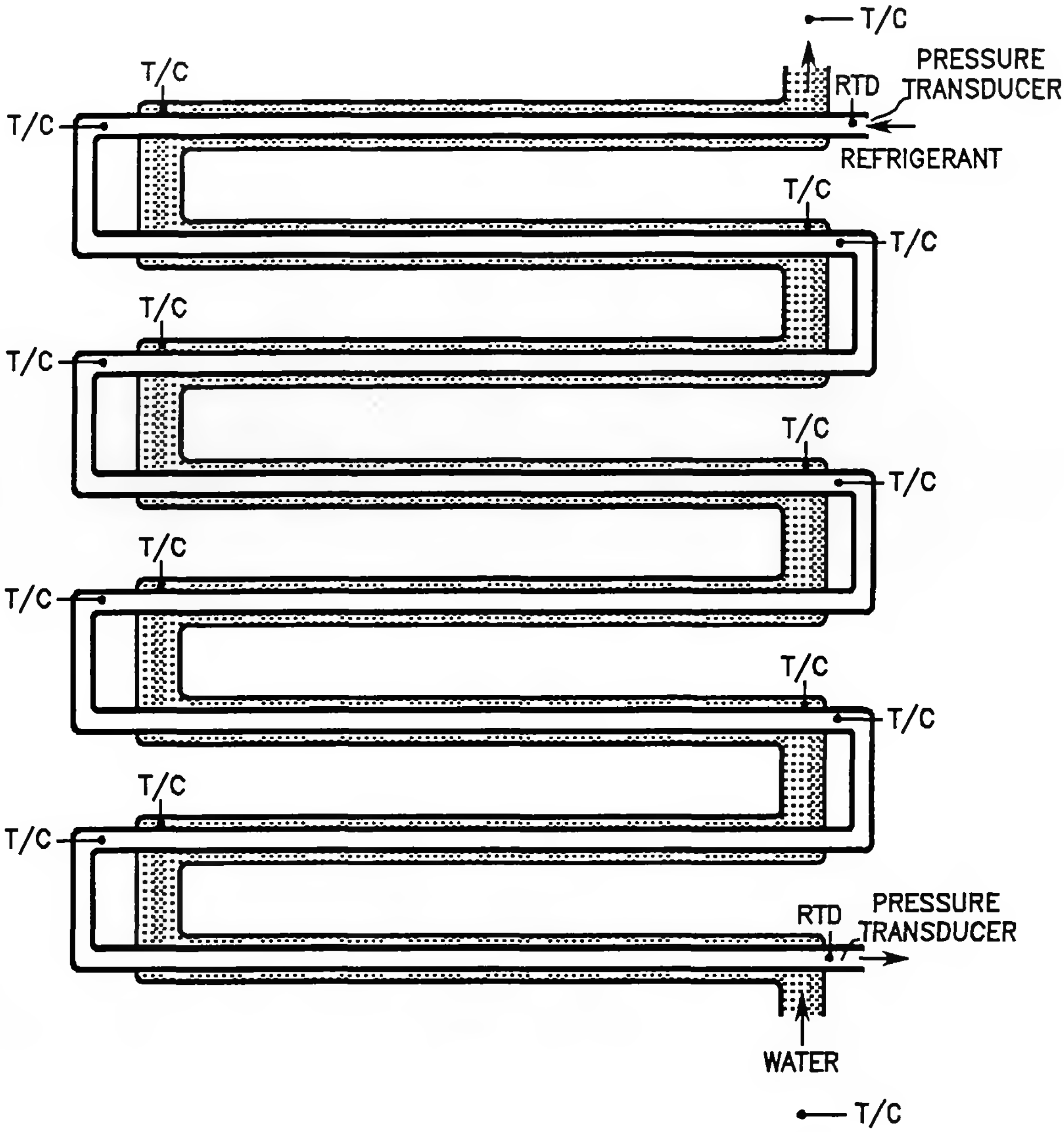

Figure 2. Heat exchanger schematic

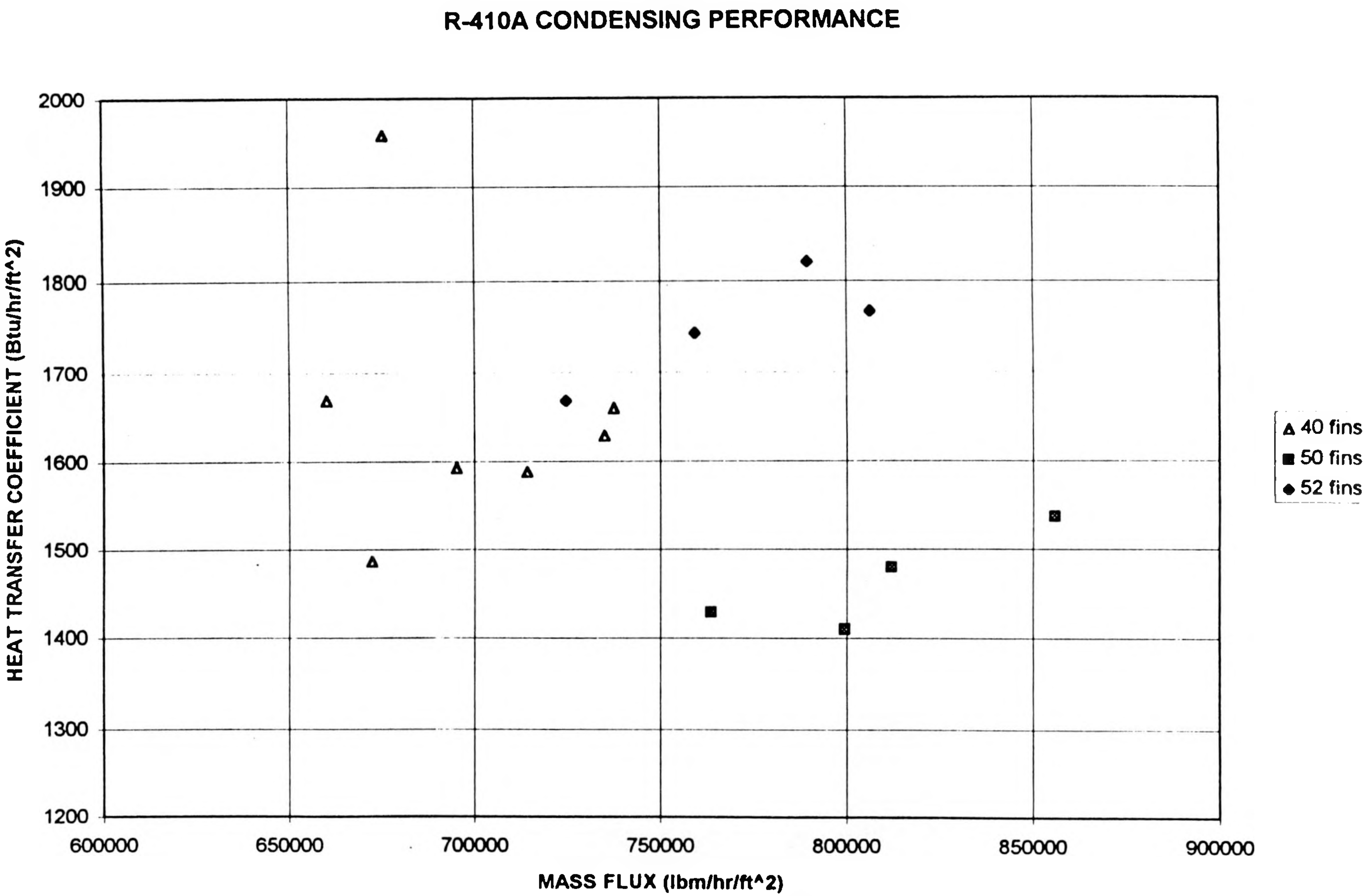

Figure 3. R-410A Condensing Performance

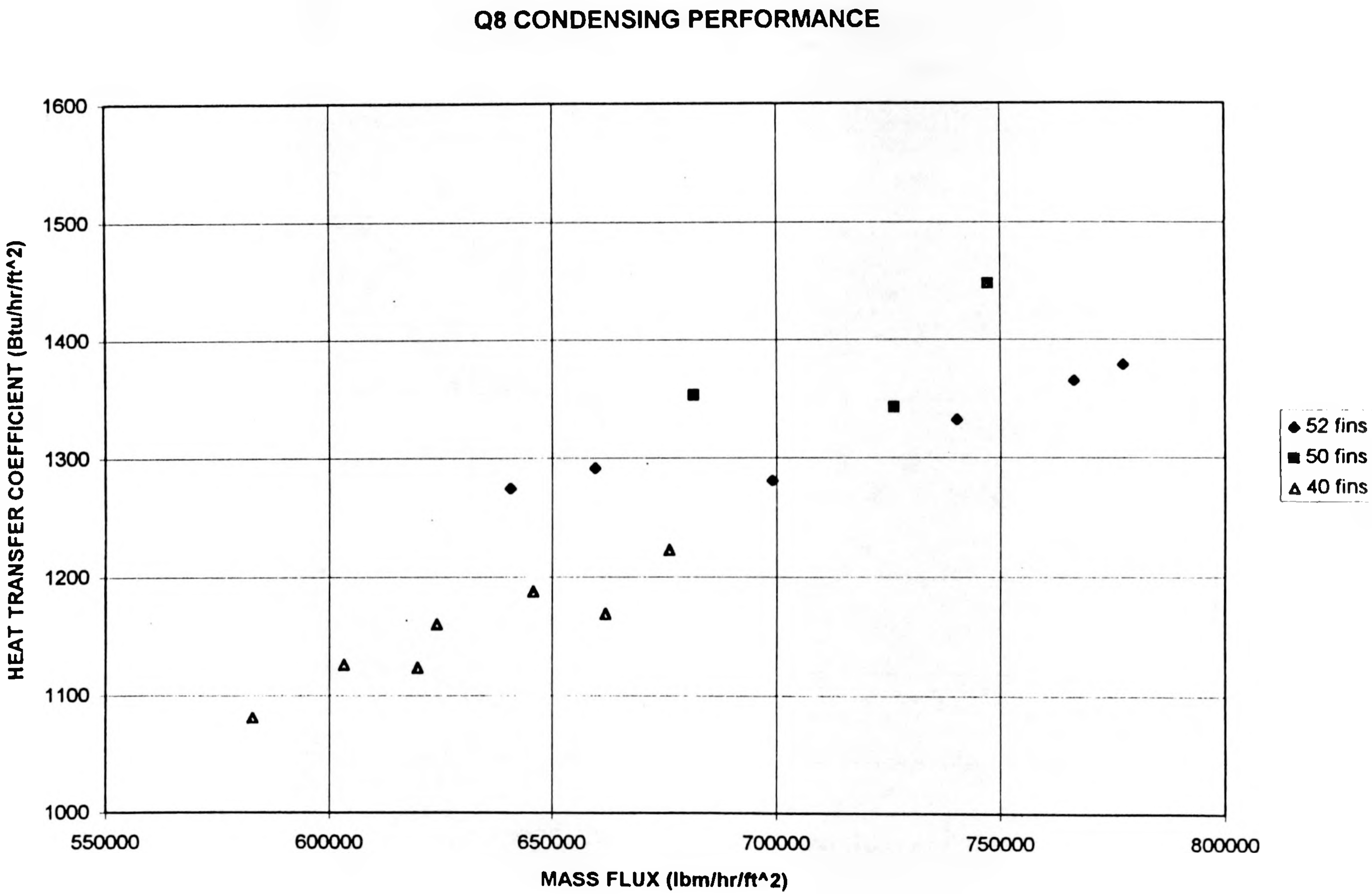

Figure 4. Q8 Condensing Performance

12

PROTECTED CRADA INFORMATION

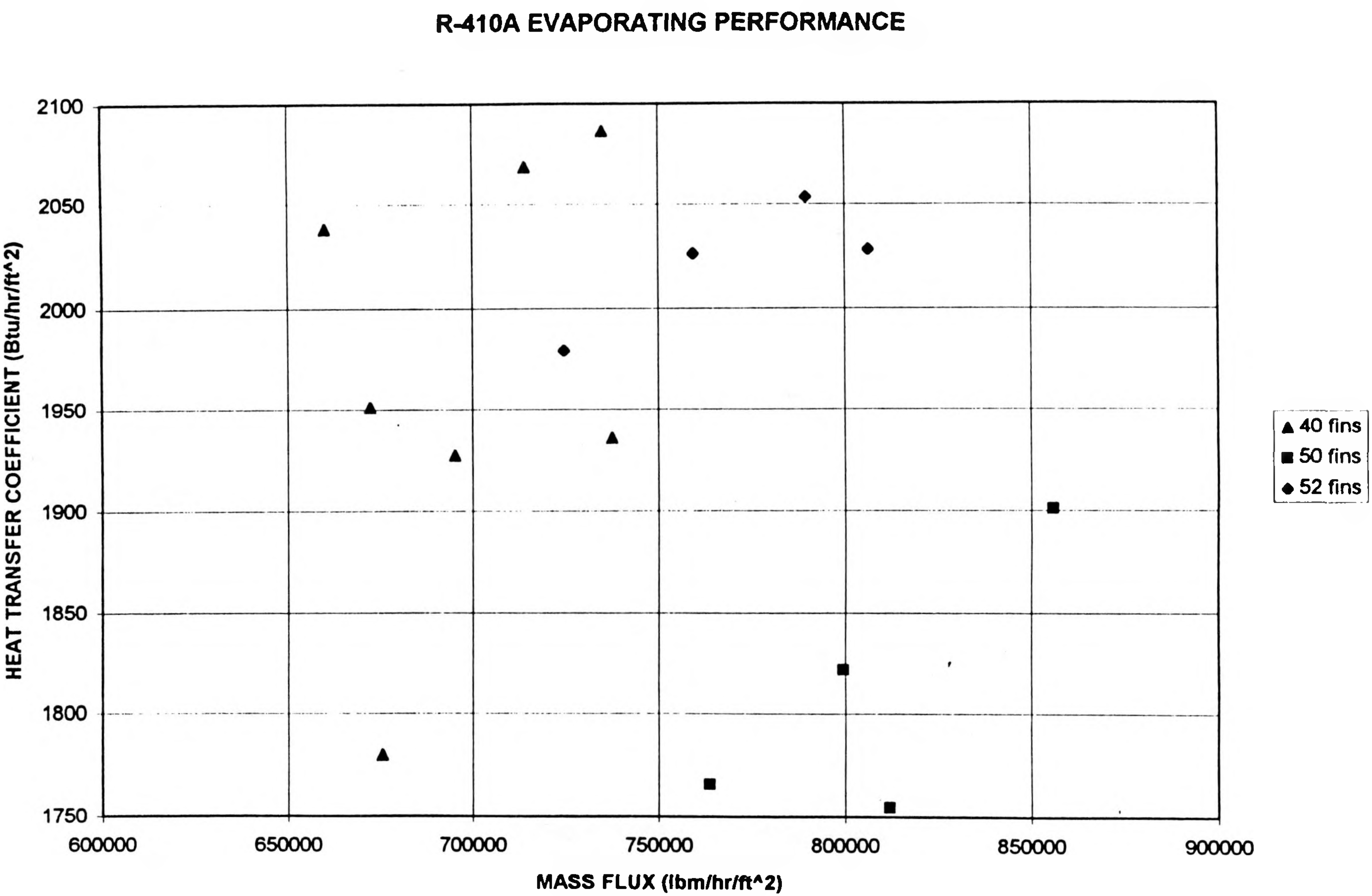

Figure 5. R-410A Evaporating Performance

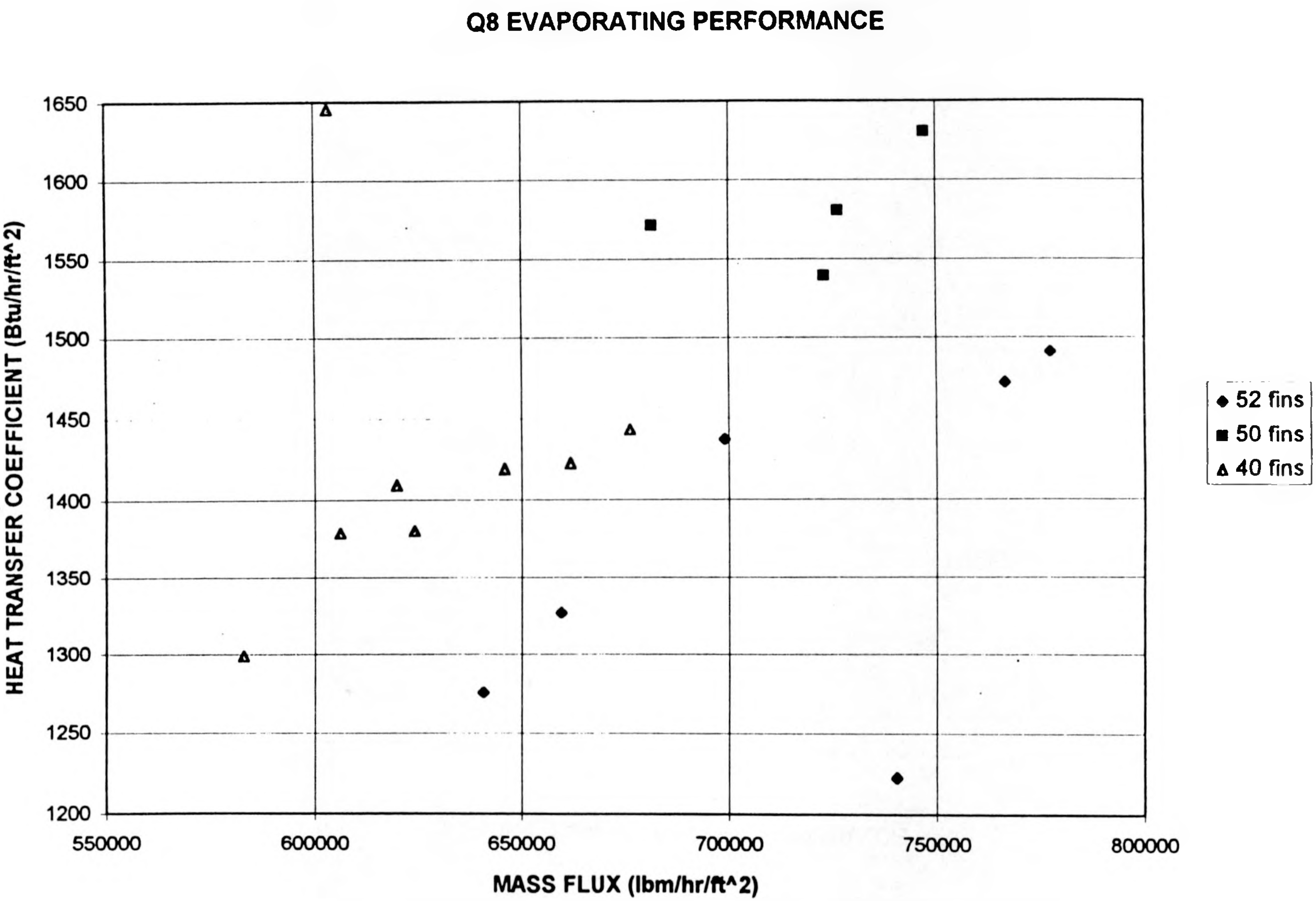

Figure 6. Q8 Evaporating Performance